Available online at www.sciencedirect.com
SCIENCE DIRECT
Bioorganic & Medicinal Chemistry 14 (2006) 2498–2506
Bioorganic & Medicinal Chemistry

Synthesis and biological evaluation of dimeric cinnamaldehydes as potent antitumor agents

Dae-Seop Shin,[a,b,†] Jong-Han Kim,[a,†] Su-Kyung Lee,[a] Dong Cho Han,[a] Kwang-Hee Son,[a] Hwan-Mook Kim,[a] Hyae-Gyeong Cheon,[c] Kwang-Rok Kim,[c] Nack-Do Sung,[d] Seung Jae Lee,[d] Sung Kwon Kang[d,*] and Byoung-Mog Kwon[a,b,*]

[a]*Korea Research Institute of Bioscience and Biotechnology, 52 Uendong Yoosung, Taejeon 305-600, Republic of Korea*
[b]*Biomolecular Science, University of Science and Technology in Korea, Taejeon 305-600, Republic of Korea*
[c]*Korea Research Institute of Chemical Technology, Taejon 305-600, Republic of Korea*
[d]*Chungnam National University, Taejon 305-764, Republic of Korea*

Received 30 September 2005; revised 14 November 2005; accepted 15 November 2005
Available online 15 December 2005

Abstract—It has been reported that 2-hydroxycinnamaldehyde and 2-benzoyl-oxycinnamaldehyde inhibited the activity of farnesyl protein transferase, angiogenesis, cell–cell adhesion, and tumor growth in vivo model. In order to improve its anti-tumor activity, dimeric cinnamaldehydes have been synthesized based on 2-hydroxycinnamaldehyde. The synthesized compounds strongly inhibited the growth of human colon tumor cells with GI_{50} values of 0.6–10 μM. Especially, 2-piperazine derivative blocked in vivo growth of human colon tumor xenograft in nude mice at 10 mg/kg. It was found that their anti-tumor effects induce apoptosis and cell cycle arrest at G_2/M phase by the compounds. It was confirmed by detection of apoptosis markers such as activated caspase-3 and cleaved PARP, and cell cycle analysis. The dimeric compounds also inhibited Cdc25B phosphatase which is essential for preinitiating G_2/M transition and S phase progression.

1. Introduction

Cinnamomum cassia Blume (Lauraceae) has been used as a spice and tea in the whole world and considered to have pharmacological properties.[1] Oil extracted from *Cinnamomum cassia* had been shown to inhibit the growth of molds[2] and exhibit cytotoxicity against human cancer cells.[3] This antitumor effect has been attributed to cinnamaldehydes such as 2-methoxycinnamaldehyde and 2-hydroxycinnamaldehyde (HCA). Various essential oils of *C. cassia* were identified by the GC–MS analysis and their biological properties studied.[4] Also, it was reported that cinnamaldehyde induces apoptosis by reactive oxygen species (ROS)-mediated mitochondrial permeability transition in human promyelocytic leukemia HL-60 cells.[5] In our previous study, we found that the antitumor effect by 2-benzoyloxycinnamaldehyde (BCA) was due to induction of reactive oxygen species.[6] Previously, we reported that HCA inhibited farnesyl protein transferase activity,[7] angiogenesis,[8] and CDK4/cyclinD1 kinase.[9] HCA and BCA also have been shown to inhibit the growth of human cancer cell lines including breast, leukemia, ovarian, lung, and colon tumor cells.[3,6] Also, CB403, one of cinnamaldehyde derivatives, was reported to inhibit tumor growth through the cell cycle arrest at G_2/M phase.[10]

Cdc25B phosphatase has been thought as a potential human oncogene, because it is essential protein for the G_2/M phase transition in human cells.[11,12] In human cells, Cdc25 phosphatases are encoded by a multigene family consisting of Cdc25A, Cdc25B, and Cdc25C.[13–15] Each Cdc25 phosphatase stimulates progression through the cell cycle by activating cyclin and CDK complexes. Cdc25C dephosphorylates and activates the mitotic kinase Cdc2/cyclin B, which is required for entry into mitosis.[16] Cdc25A is important for entry into S phase,[17] whereas Cdc25B is essential for preinitiating G_2/M transition and S phase progression.[12] Cdc25B is thought to function as a mitotic starter by dephosphorylating and activating Cdk2/cyclin A and Cdk1/cyclin B.[18] Because of these reasons,

Keywords: Cinnamaldehyde; Dimeric cinnamaldehyde; Apoptosis; Cell cycle; Cdc25B phosphatase.
* Corresponding authors. Tel.: +82 42 860 4557; fax: +82 42 861 2675; e-mail addresses: skkang@cnu.ac.kr; kwonbm@kribb.re.kr
† These authors contributed equally to this work.

0968-0896/$ - see front matter © 2005 Elsevier Ltd. All rights reserved.
doi:10.1016/j.bmc.2005.11.028

identification of Cdc25B inhibitors becomes an active area for the development of antitumor agents.

In this study, we evaluated the biological activity of dimeric cinnamaldehyde as a potent anti-tumor agent. Inhibitory activity of Cdc25B of the synthesized compounds was also examined, because the compounds arrested the cell cycle at the G_2/M phase in tumor cells. Especially, we focused on two types of dimeric cinnamaldehyde derivatives such as 2-(4-Br-benzyl)-dimer (**11**) and 2-(*N*-CH_3-piperazine)-dimer (**21**).

2. Results and discussion

2.1. Chemistry

As shown in Scheme 1, the cinnamaldehyde derivatives are prepared by linear dimerization of benzaldehyde substituted by R_1, R_2, and R_3 in the presence of 2,5-dimethoxytetrahydrofuran, potassium acetate, acetic acid, and water (wherein, R_1, R_2, and R_3 are described in Table 1).[19,20] The benzaldehydes substituted with R_1, R_2 and, R_3 are used as commercially available formulation. Also, the benzaldehydes substituted with R_1, R_2, and R_3 are prepared by reacting alkylating agents to benzaldehyde substituted with activating substituent such as halogen or hydroxy group in the presence of base. For example, 2-*n*-propyloxybenzaldehyde was prepared by reacting 1-iodopropane (alkylating agent) to 2-hydroxybenzaldehyde substituted with hydroxyl group in the presence of potassium carbonate. To improve the solubility in water, 2-(*N*-CH_3-piperazine)-dimer (**21**) was synthesized by the described method. The solubility of compound **21** is 0.2 mg/mL in water and it is freely soluble in acidic water (pH 3). We also tried to synthesize of 2-hydroxy dimeric cinnamaldehyde, unfortunately, we could not obtain the dimeric compound. As shown in Scheme 1, the 2-hydroxyl group reacted with the aldehyde carbonyl group to give a cyclic compound **22**.

2.1.1. X-ray structure of cinnamaldehyde dimers and a cyclic product. The crystallized compounds **3**, **17**, and **22** were obtained from acetone–hexane to confirm the structure and to see three-dimensional shape of the synthesized compounds. X-ray analysis of the crystallized compounds **3** and **17** confirmed the proposed structure with a linear dimeric system. The X-ray structures of **3** and **17** show that the aldehyde groups are on the same plane in the solid state (Fig. 1). X-ray analysis of the crystallized compound **22** obtained from acetone–hexane confirmed the proposed structure with a unique fused ring system.

2.2. Inhibition of Cdc25B activity by dimeric cinnamaldehydes

Cdc25B is an essential protein for the G_2/M phase transition in various human cancer cell lines.[11,12] Therefore, inhibition of Cdc25B causes cell cycle arrest leading to suppression of tumor growth. In our previous study, it was shown that cinnamaldehyde derivatives, CB403, induced cell cycle arrest at G_2/M phase.[10] Therefore, we primarily examined the inhibitory activity of Cdc25B by dimeric cinnamaldehydes. The dimeric cinnamaldehydes such as **4**, **9**, **10**, and **11** strongly and selectively inhibited Cdc25B activity with IC_{50} values of less than 10 μM (Table 2).

2.3. Inhibition of human colon tumor cell growth by dimeric cinnamaldehydes

In order to investigate whether the dimeric cinnamaldehydes inhibit cancer cell proliferation, HCT116 and SW620 (human colon tumor cells) were treated at

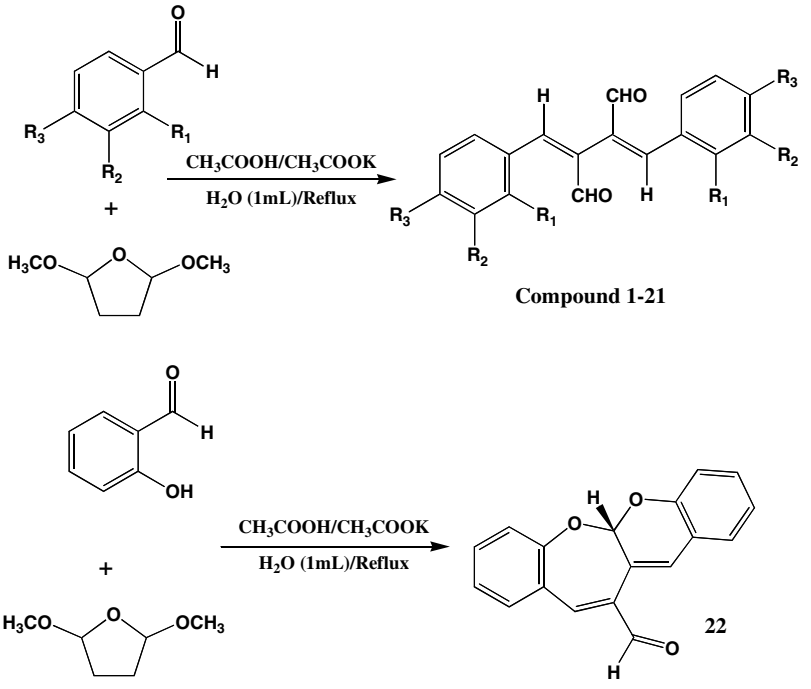

Scheme 1. Synthesis of dimeric cinnamaldehydes **1**–**21** and compound **22**.[19]

Table 1. Synthesized dimeric cinnamaldehydes

Compound	R_1	R_2	R_3	Mp (°C)
1	–H	–H	–H	150–151
2	–F	–H	–H	141–142
3	–Cl	–H	–H	177–178
4	–Br	–H	–H	194–195
5	$-OCH_3$	–H	–H	163–164
6	$-OCH_2CH_2CH_3$	–H	–H	109–110
7	$-OCH_2CHCH_2$	–H	–H	117–118
8	$-OCH(CH_3)_2$	–H	–H	109–110
9	$-OCH_2C_6H_5$	–H	–H	120–121
10	$-OCH_2C_6H_4$–4-Cl	–H	–H	186–187
11	$-OCH_2C_6H_4$-4-Br	–H	–H	210–211
12	$-OCH_2C_6H_4$–4-NO_2	–H	–H	116–117
13	–H	–Cl	–H	107–108
14	–H	$-OCH_2CH_2CH_3$	–H	93–94
15	–H	$-OCH(CH_3)_2$	–H	116–117
16	–H	$-OCH_2C_6H_5$	–H	126–127
17	–H	$-OCH_3$	–OH	177–178
18	–H	$-OCH_3$	$-OCH_3$	149–150
19	–H	$-OCH_3$	$-OCH_2CH_2CH_3$	95–96
20	–H	$-OCH_3$	$-OCH(CH_3)_2$	119–120
21	–Piperazine-*N*-CH_3	–H	–H	118–220

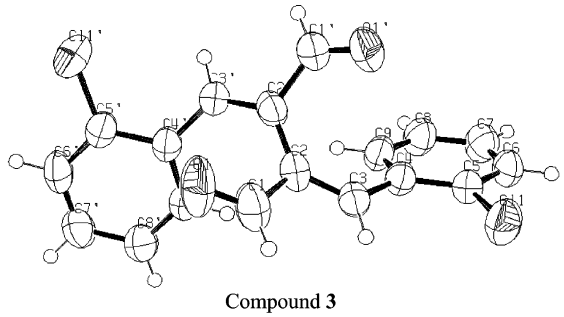

Compound **3**

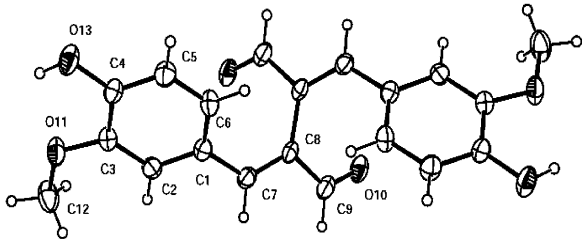

Compound **17**

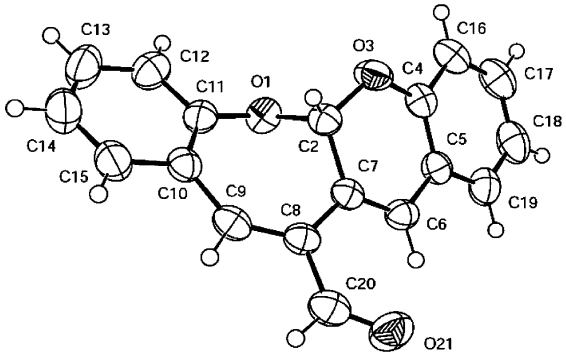

Compound **22**

Figure 1. ORTEP drawing of the X-ray structure of compounds **3**, **17**, and **22**.

different concentrations from 0.1 to 100 μM for 24 h (Table 3). Both these tumor cells were inhibited by the compounds with a GI_{50} value of 0.6–10 μM.

As shown in Figure 2, 2-(4-Br-benzyl)-dimer (**11**) and 2-(*N*-CH_3-piperazine)-dimer (**21**) exhibited a dose-dependent inhibition of tumor cell growth in a broad range of concentrations and the GI_{50} value of **21** for in vitro growth inhibition was approximately 2.8 μM for MDA-MB-231 (human breast cancer cell) and 2.1 μM for SW620 cells. It was also found that morphology of two cell lines was changed at the concentration of 5 μM

Table 2. Inhibitory activity of dimeric cinnamaldehydes against phosphatase

Compound	Cdc25B		% inhibition (at 10 μM)	
	% inhibition (at 10 μM)	IC_{50} (μM)	Cdc25A	PTP-1B
1	6.70			
2	5.99			
3	39.07		11.80	2.63
4	56.21	7.79	25.70	5.63
5	1.10			
6	29.95			
7	6.26			
8	7.97			
9	60.49	7.08	8.85	1.80
10	89.56	4.77	6.74	2.87
11	95.00	1.94	19.24	7.49
12	1.31			
13	28.41			
14	22.80			
15	2.25			
16	55.16	14.66	11.61	1.86
17	5.60			
18	9.34			
19	9.84			
20	3.08			
21	5.33			

Table 3. The effects of dimeric compounds on tumor cell growth

No.	Compound	HCT116 GI_{50} (μM)	SW620 GI_{50} (μM)
1	H	8.39	1.52
2	2-F	4.02	10.73
3	2-Cl	0.91	0.91
4	2-Br	1.05	2.14
5	2-OCH_3	3.72	1.55
6	2-*n*-Propyl	5.28	2.11
7	2-*i*-Propyl	5.28	2.64
8	2-Allyl	5.34	5.34
9	2-Benzyl	1.41	0.63
10	2-(4-Cl-benzyl)	0.84	0.54
11	2-(4-Br-benzyl)	2.63	4.64
12	2-(4-NO_2-benzyl)	5.19	7.09
13	3-Cl	3.62	9.21
14	3-*n*-Propyl	2.74	6.74
15	3-*i*-Propyl	4.23	0.61
16	3-Benzyl	7.59	3.58
17	4-OH, 5-OCH_3	7.87	3.53
18	3,4-OCH_3	5.49	10.46
19	3-OCH_3, 4-*n*-propyl	0.62	2.28
20	3-OCH_3, 4-*i*-propyl	0.71	0.91
21	2-Piperazine-*N*-CH_3	3.88	6.22

of 2-(4-Br-benzyl)-dimer (**11**) and 2-(*N*-CH_3-piperazine)-dimer (**21**) (Fig. 3). Unfortunately, new cyclic compound **22** did not inhibit the growth of human tumor cells.

2.4. Effects of 2-(*N*-CH_3-piperazine)-dimer 21 on the cell cycle of cancer cells

To determine the effects of 2-(*N*-CH_3-piperazine)-dimer (**21**) on the cell cycle, after treatment of the compound (5 μM) in SW620 cells, the cells were harvested and analyzed with a FACScalibur. As shown in Figure 4. 2-(*N*-CH_3-piperazine)-dimer (**21**) arrested the progression of the cells at G_2/M phase.

2.5. 2-(4-Br-benzyl)-dimer (11) and 2-(*N*-CH_3-piperazine)-dimer (21) induce apoptosis in MDA-MB-231 and SW620 cells

To determine whether the growth inhibition by two dimeric cinnamaldehydes was associated with apoptosis, Western blot analysis of PARP and cleavage caspase-3 was performed (Fig. 5). The PARP and cleavage caspase-3 was enhanced by 10 μM of 2-(*N*-CH_3-piperazine)-dimer (**21**) in MDA-MB-231 cells, although we could not detect any significant increase of PARP or caspase-3 over 10 μM (Fig. 5A left panel). However, remarkable increase of PARP and cleavage caspase-3 was shown by 5 μM of 2-(4-Br-benzyl)-dimer (**11**) (Fig. 5A right panel). Although, a trace amount of PARP degradation and cleavage caspase-3 was observed in 2-(*N*-CH_3-piperazine)-dimer (**21**)-treated cells, these results state that the dimeric compounds inhibited cancer cell growth through apoptosis.

2.6. In vivo effect of 2-(*N*-CH_3-piperazine)-dimer 21 on tumor cell growth

SW620 tumor xenograft model of nude mice was used to investigate the inhibitory activity of the compound **21** on tumor growth. SW620 cells were implanted subcutaneously into the right flank of nude mice on day 0 and compound was intraperitoneously administered at a concentration of 10 mg/kg per day for 20 days. To determine the toxicity of the compound, the body weight of tumor-bearing animals was measured. The mice were sacrificed and the tumors were weighed on day 20. Tumor volume was decreased by 45.6% compared to control mice. Twenty days after implantation (Fig. 6), tumor weights were also decreased by 50.2% compared to control mice in SW620 cells. Body weight loss was not observed in mice implanted with SW620 cells (data not shown).

3. Conclusion

Cinnamaldehydes have been known to have antitumor activity.[5,6] However, the mechanism is still in debate. In our previous study, we reported that cinnamaldehyde derivatives have an inhibitory activity against FPTase[7] and induce reactive oxygen species[6] that may (at least in part) explain the mechanism by which cinnamaldehydes exhibit their antitumor activity. In this study, we showed that growth inhibition of tumor cells was in-

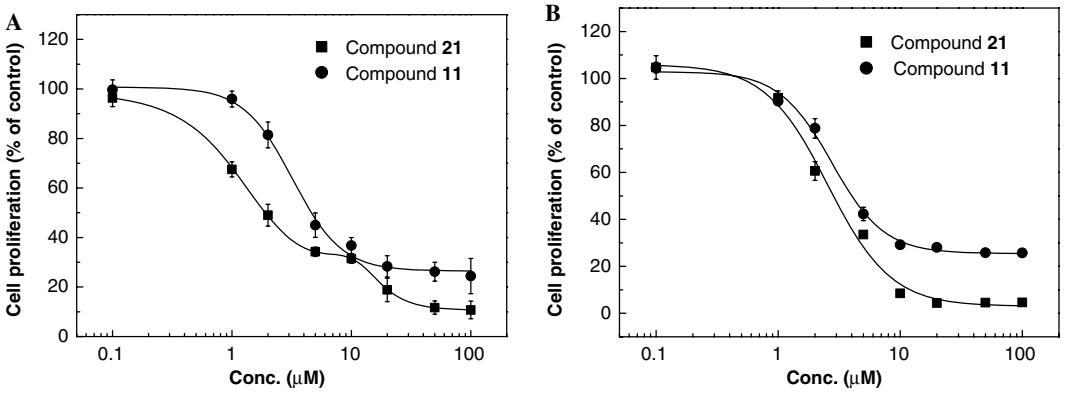

Figure 2. Growth inhibition of cancer cells by 2-(4-Br-benzyl)-dimer (**11**) and 2-(*N*-CH_3-piperazine)-dimer (**21**). Compounds were treated in MDA-MB-231 (A) and SW620 (B) cell line with different concentrations of the compounds. Viability was determined by WST-1 at 24 h after compound treatment.

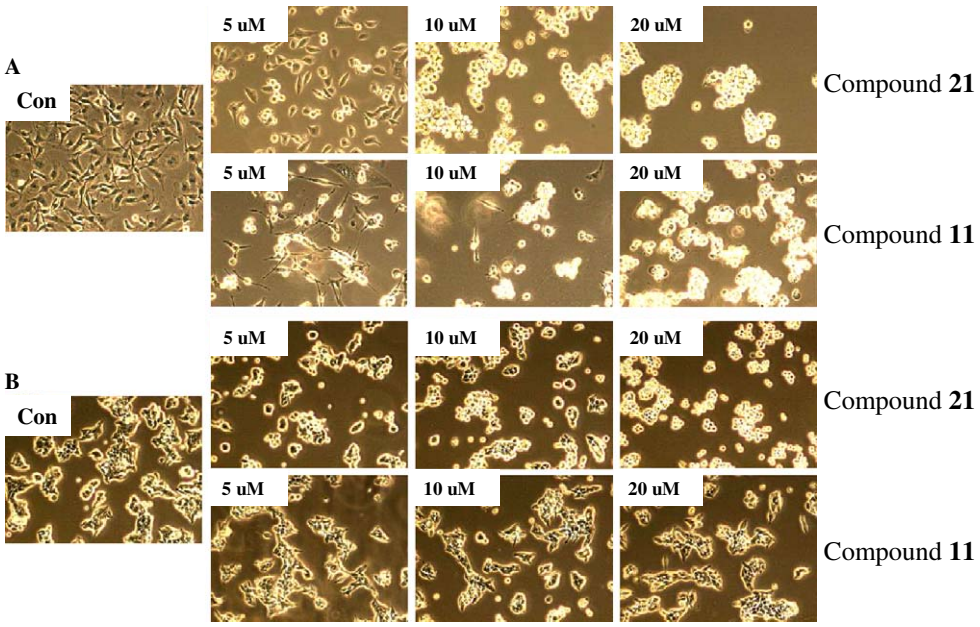

Figure 3. Morphology change by compound **11** and **21**. MDA-MB-231 (A) and SW620 (B) cells were imaged by Nikon fluorescence microscope after 24 h from compound treatment.

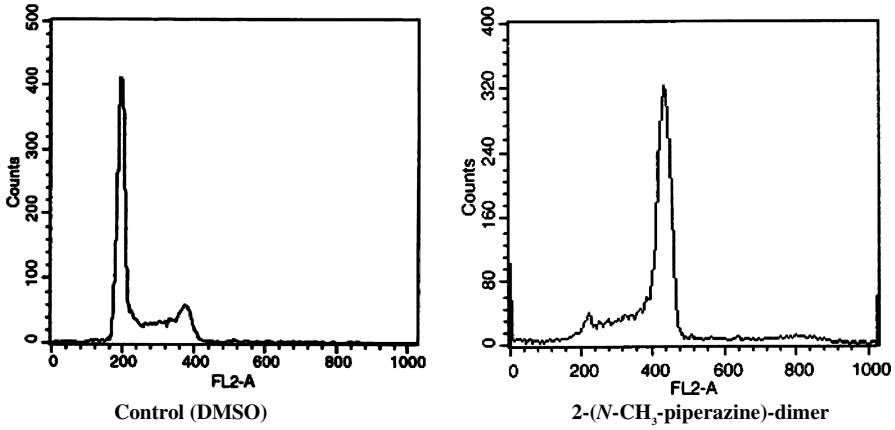

Figure 4. Effects of 2-(*N*-CH_3-piperazine)-dimer (**21**) on cell cycle. SW620 cells were treated with 2-(*N*-CH_3-piperazine)-dimer (**21**). Cells were harvested after 24 h and were subjected to FACScalibur analysis to determine the distribution of cells through the G_1, S, and G_2/M phases. Experiments were performed at least three times with consistent and repeatable results.

duced by the dimeric cinnamaldehydes through PARP degradation via caspase-3 pathway or cell cycle arrest in G_2/M phase. A SW620 tumor xenograft model of nude mice was used to investigate the inhibitory activity on tumor growth by **21**, which was intraperitoneously administered at concentrations of 10 mg/kg from day 1 to day 20. As shown in Fig. 6, compound **21** inhibited the growth of tumors and also significantly reduced the weight of tumors. A promising aspect of **21** is apparent lack of obvious toxicity in tumor-bearing nude mice. Therefore, the dimeric cinnamaldehyde derivative exerts antitumor effects by inducing G_2/M phase arrest in cancer cells and also apoptosis of tumor cells. The growth inhibitory activity of the compounds in cells and animal studies supports their promise as anti-tumor compounds.

4. Experimental

4.1. Materials and methods

NMR spectra were measured at 300 and 400 MHz (^{1}H and ^{13}C), and chemical shifts are reported relative to internal Me_4Si. Melting points are reported in degrees Celsius and are uncorrected. Thin-layer chromatography was effected on silica gel 60 F254 (layer thickness 0.2 mm), and components were located by observation under UV light and/or by treating the plates with a *p*-anisaldehyde reagent followed by heating. Flash chromatography was performed on Merck silica gel, 60 and 230–400 mesh by Still's methods.[20]

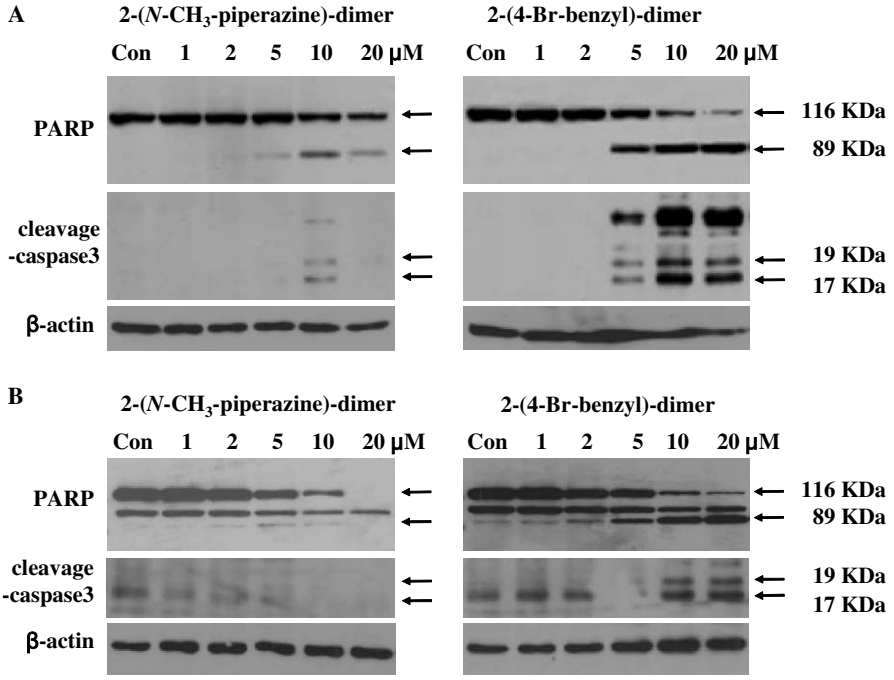

Figure 5. Induction of PARP and cleavage caspase-3 by dimeric cinnamaldehydes. 2-(4-Br-benzyl)-dimer (**11**) and 2-(*N*-CH_3-piperazine)-dimer (**21**) were treated in MDA-MB-231 and SW620 cells. Cell lysates were prepared with RIPA buffer after 24 h and 40 μg of lysates was resolved by SDS–PAGE. Western blot analysis of PARP and cleaved caspase-3 was carried with each MDA-MB-231 (A) or SW620 cell lysate (B).

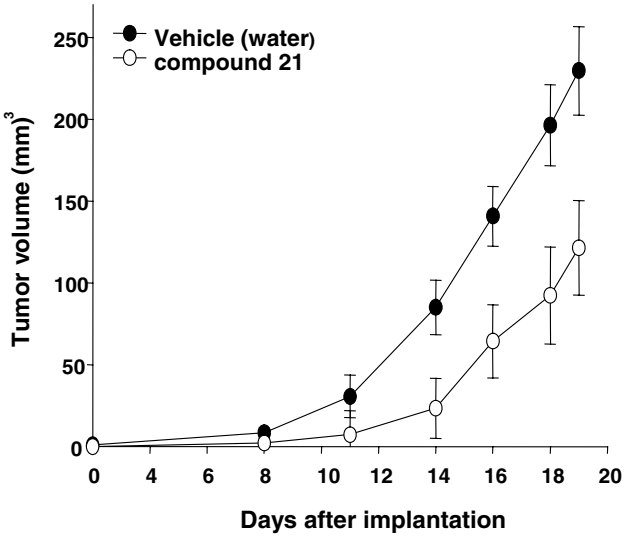

Figure 6. Tumor volume change of SW620 xenografted nude mice treated with compound **21**. For the evaluation of in vivo antitumor activity of compound **21**, SW620 (0.3 mL of 3×10^7 cells/mL) was implanted subcutaneously into the right flank of nude mice on day 0. Tumor volumes were estimated by the formula length (mm) × width (mm) × height (mm)/2. Compounds were dissolved in water and intraperitoneally administered at the concentration of 10 mg/kg per day from day 1 to 20. Error bar is standard deviation.

4.2. Synthesis of dimeric cinnamaldehydes

4.2.1. 2,3-Bis-benzylidenesuccinaldehyde (1). A mixture of 2,5-dimethoxytetrahydrofuran (2 mL, 15 mmol), benzaldehyde (30 mmol), acetic acid (1 mL), water (1 mL), and potassium acetate (2 g) was heated under reflux for 12 h. After cooling, the mixture is poured into water. The mixture is extracted with chloroform, the extract is washed with water, dried ($MgSO_4$), and evaporated, which was purified by column chromatography. Yield = 13%, ^{1}H NMR ($CDCl_3$/TMS): δ 7.26–7.53 (m, 10H), 7.71 (s, 2H), 9.67 (s, 2H).

4.2.2. 2,3-Bis-(2-fluorobenzylidene)succinaldehyde (2). Yield = 10%, ^{1}H NMR ($CDCl_3$/TMS): δ 7.0 (m, 4H), 7.29 (m, 4H), 7.88 (s, 2H), 9.69 (s, 2H).

4.2.3. 2,3-Bis-(2-chlorobenzylidene)succinaldehyde (3). Yield = 14%, ^{1}H NMR ($CDCl_3$/TMS): δ 7.13–7.28 (m, 8H), 7.83 (s, 2H), 9.73 (s, 2H).

4.2.4. 2,3-Bis-(2-bromobenzylidene)-succinaldehyde (4). Yield = 10%, ^{1}H NMR ($CDCl_3$/TMS) δ 7.12–7.46 (m, 8H), 7.73 (s, 2H), 9.74 (s, 2H).

4.2.5. 2,3-Bis-(2-methoxybenzylidene)succinaldehyde (5). Yield = 15%, ^{1}H NMR ($CDCl_3$/TMS): δ 3.85 (s, 6H), 6.76 (m, 4H), 7.5 (m, 2H), 7.4 (dd, 2H, J = 1.2, 7.5 Hz), 8.07 (s, 2H), 9.65 (s, 2H).

4.2.6. 2,3-Bis-(2-*n*-propyloxybenzylidene)succinaldehyde (6). A solution of 6.1 g (50 mmol) of 2-hydroxybenzaldehyde in 50 mL of acetonitrile was stirred with K_2CO_3 (60 mmol, 8.28 g) and 1-iodopropane (55 mmol, 9.35 g) under reflux, and the progress of the reaction was monitored by TLC. When TLC indicated the disappearance of starting material, the reaction was stopped. The reaction mixture was then cooled to room temperature, quenched with water, and extracted with ethyl acetate. The organic layer was washed with water, dried over

anhydrous $MgSO_4$, filtered, and concentrated. Purification by column chromatography over silica gel afforded the corresponding products **6**. Yield = 10%, ^{1}H NMR ($CDCl_3$/TMS): δ 1.08 (t, 6H, J = 7.5 Hz), 1.86 (m, 4H), 3.96 (m. 4H), 6.76 (m, 2H), 6.83 (d, 2H, J = 7.5 Hz), 7.26 (m, 2H), 7.42 (dd, 2H, J = 1.2, 7.5 Hz), 8.12 (s, 2H), 9.66 (s, 2H).

4.2.7. 2,3-Bis-(2-allyloxybenzylidene)succinaldehyde (7). Yield = 10%, ^{1}H NMR ($CDCl_3$/TMS): δ 4.57 (m, 4H), 5.36 (m, 4H), 6.07 (m, 2H), 6.7 (m, 4H), 7.25 (dt, 2H, J = 1.5, 8.1 Hz), 7.41 (dd, 2H, J = 1.5, 8.1 Hz), 8.11 (s, 2H), 9.67 (s, 2H).

4.2.8. 2,3-Bis-(2-isopropyloxybenzylidene)succinaldehyde (8). Yield = 8%, ^{1}H NMR ($CDCl_3$/TMS): δ 1.38 (t, 12H, J = 6.0 Hz), 4.58 (m. 2H), 6.75 (t, 2H, J = 7.8 Hz), 6.86 (d, 2H, J = 7.8 Hz), 7.26 (dt, 2H, J = 1.8, 7.8 Hz), 7.43 (dd, 2H, J = 1.8, 7.8 Hz), 8.11 (s, 2H), 9.66 (s, 2H).

4.2.9. 2,3-Bis-(2-benzyloxybenzylidene)succinaldehyde (9). Yield = 10%, ^{1}H NMR ($CDCl_3$/TMS): δ 5.09 (dd, 4H, J = 1.2, 9.0 Hz), 6.78 (t, 2H, J = 7.8 Hz), 6.88 (d, 2H, J = 7.8 Hz), 7.26 (dt, 2H, J = 1.8, 7.8 Hz), 7.26 (m, 12H), 8.13(s, 2H), 9.65 (s, 2H).

4.2.10. 2,3-Bis-{2-(4-chlorobenzyloxy)benzylidene}succinaldehyde (10). Yield = 8%, ^{1}H NMR ($CDCl_3$/TMS); δ 5.02 (dd, 4H, J = 1.2, 9.0 Hz), 6.73 (t, 2H, J = 7.8 Hz), 6.78 (d, 2H, J = 7.8 Hz), 7.32 (m, 14H), 8.01 (s, 2H), 9.56 (s, 2H).

4.2.11. 2,3-Bis-{2-(4-bromobenzyloxy)benzylidene}succinaldehyde (11). Yield = 15%, ^{1}H NMR ($CDCl_3$/TMS): δ 5.07 (dd, 4H, J = 1.2, 9.0 Hz), 6.82 (m, 4H), 7.32 (m, 8H), 7.41 (dd, J = 1.8, 7.8 Hz), 8.08 (s, 2H), 9.63 (s, 2H).

4.2.12. 2,3-bis-{2-(4-nitrobenzyloxy)benzylidene}succinaldehyde (12). Yield = 9%, ^{1}H NMR ($CDCl_3$/TMS): δ 5.31 (s, 4H), 7.01 (d, 2H, 7.5 J = 7.5 Hz), 7.10 (t, 2H, J = 7.5 Hz), 7.55 (dt, 2H, J = 1.5, 7.5 Hz), 7.63 (d, 4H, 7.7 Hz), 7.88 (dd, 2H, J = 1.5, 7.5 Hz), 8.27 (d, 4H, 7.7 Hz), 10.56 (s, 2H).

4.2.13. 2,3-Bis-(3-chlorobenzylidene)succinaldehyde (13). Yield = 15%, ^{1}H NMR ($CDCl_3$/TMS): δ 7.24 $\sim$ 7.42 (m, 8H), 7.64 (s, 2H), 9.67 (s, 2H).

4.2.14. 2,3-Bis-(3-*n*-propyloxybenzylidene)succinaldehyde (14). Yield = 10%, ^{1}H NMR ($CDCl_3$/TMS): δ 0.99 (t, 6H J = 7.2 Hz), 1.76 (m, 4H), 3.81 (dt, 4H, J = 1.2, 6.6 Hz), 7.22 (m, 8H), 7.67 (s, 2H), 9.65 (s, 2H).

4.2.15. 2,3-Bis-(3-isopropyloxybenzylidene)succinaldehyde (15). Yield = 10%, ^{1}H NMR ($CDCl_3$/TMS): δ 1.27 (dd, 12H, J = 5.7, 15.4 Hz), 4.39 (m, 2H), 7.16 (m, 8H), 7.66 (s, 2H), 9.65 (s, 2H).

4.2.16. 2,3-Bis-(3-benzyloxybenzylidene)succinaldehyde (16). Yield = 10%, ^{1}H NMR ($CDCl_3$/TMS): δ 4.97 (s, 4H), 7.01 (m, 6H), 7.25 (m, 12H), 7.51 (s, 2H), 9.48 (s, 2H).

4.2.17. 2,3-Bis-(4-hydroxy-3-methoxybenzylidene)succinaldehyde (17). Yield = 10%, ^{1}H NMR ($CDCl_3$/TMS) (ppm); δ 3.75 (s, 6H), 5.92 (s, 2H), 7.10 (m, 6H), 7.63 (s, 2H), 9.63 (s, 2H).

4.2.18. 2,3-Bis-(3,4-dimethoxybenzylidene)succinaldehyde (18). Yield = 15%, ^{1}H NMR ($CDCl_3$/TMS): δ 6.73 (s, 6H), 3.88 (s, 6H), 6.82 (d, 2H, J = 8.1 Hz), 7.11 (d, 2H, J = 1.8 Hz), 7.19 (dd, J = 1.8, 8.1 Hz), 7.65 (s, 2H), 9.65 (s, 2H).

4.2.19. 2,3-Bis-(3-methoxy-4-*n*-propyloxybenzylidene)succinaldehyde (19). Yield = 75%, ^{1}H NMR ($CDCl_3$/TMS): δ 1.01 (t, 6H, J = 7.2 Hz), 1.84 (m, 4H), 3.70 (s, 6H), 3.97 (t, 4H, J = 6.6 Hz), 6.80 (d, 2H, J = 8.4 Hz), 7.11 (d, 2H, J = 1.8 Hz), 7.19 (dd, J = 1.8, 8.4 Hz), 7.63 (s, 2H), 9.64 (s, 2H).

4.2.20. 2,3-Bis-(3-methoxy-4-isopropyloxybenzylidene)succinaldehyde (20). Yield = 80%, ^{1}H NMR ($CDCl_3$/TMS): δ 1.36 (d, 12H, J = 6.0 Hz), 3.69 (s, 6H), 4.57 (m, 2H), 6.82 (d, 2H, J = 8.4 Hz), 7.11 (d, 2H, J = 2.1 Hz), 7.15 (dd, 2H, J = 2.1, 8.4 Hz), 7.63 (s, 2H), 9.64 (s, 2H).

4.2.21. 2,3-Bis-(2-(4-*N*-methyl)-piperazine)succinaldehyde (21). 2-Fluorobenzaldehyde (42.16 mL, 400 mmol) was added to the 250 mL round-bottomed flask, 100 mL of dimethylformamide (DMF) was further added therein. Thereafter, 8.28 g of potassium carbonate (60 mmol) and 44.4 mL of *N*-methylpiperazine (400 mmol) were added therein. The reaction mixture was refluxed at 150 °C for 10 hr. After the reaction was terminated, the reaction mixture was cooled to room temperature. Thereafter, 400 mL of water was added to the reaction mixture. The reaction mixture was extracted with 200 mL of ethyl acetate three times. The ethyl acetate layers were collected, washed with water three times, and dried with anhydrous magnesium sulfate. The ethyl acetate was removed under reduced pressure. The resulting residue was purified with column chromatography, to give 2-(4-*N*-methylpiperazine)benzaldehyde.

2-(*N*-CH_3-piperazine)benzaldehyde (4.5 g, 30 mmol) prepared in the above step was dissolved in 250 mL of round-bottomed flask. Thereafter, 2 mL of 2,5-dimethoxytetrahydrofuran (15 mmol), 2 g of potassium acetate (20 mmol), 1 mL of acetic acid (16 mmol), and 1 mL water were added to the flask. The reaction mixture was refluxed at 110 °C for 12 h. After the reaction was terminated, the reaction mixture was cooled to room temperature. Thereafter, water was added to the reaction mixture. The reaction mixture was extracted with 100 mL chloroform for three times. The chloroform layers were collected, washed with water for three times, and dried with anhydrous magnesium sulfate. The chloroform was removed under reduced pressure. The resulting residue was purified with column chromatography, to give the title compound as a yellow crystal (4.5 g, yield: 65%). ^{1}H NMR ($CDCl_3$/TMS): δ 2.25 (s, 6H, OCH_3), 2.40–2.85 (br d 16H), 6.94 (dt, 2H, J = 1.2, 7.5 Hz), 7.04 (dd, 2H, 2H, J = 1.2, 7.5 Hz), 7.22 (dd, 2H, J = 1.2, 7.8 Hz), 7.32 (dt, 2H, J = 1.2, 7.5 Hz), 7.92 (s, 2H), 9.70 (s, 2H).

4.2.22. Cyclic compound 22. Yield = 20%, ^{1}H NMR ($CDCl_3$/TMS): δ 5.63 (s, 1H), 7.1–7.4 (m, 8H), 7.51 (dd, 1H, J = 1.2, 6.0 Hz), 7.75 (s, 1H), 9.79 (s, 1H).

4.3. X-ray structure

The data for X-ray structure determination were collected on Bruker P4 and CAD-4 diffractometers equipped with graphite monochromated Mo Kα radiation (λ = 0.71073 Å) at 295 K. The unit cell dimensions were determined on the basis of 36 reflections in the range of $5.15° < \theta < 12.56°$ for compound **3**, 25 reflections in the range of $9.86° < \theta < 13.97°$ for compound **17**, and 23 reflections in the range of $11.41° < \theta < 12.67°$ for compound **22**. The data were collected by the $\omega/2\theta$ scan mode. The standard direct method was used to position the heavy atoms. The remaining non-hydrogen atoms were located from the subsequent difference Fourier synthesis. All non-hydrogen atoms were refined anisotropically. All hydrogen atoms were calculated in ideal positions and were riding on their respective carbon atoms ($B_{iso} = 1.2B_{eq}$ and $B_{iso} = 1.5B_{eq}$). The structure was refined in a full matrix least-squares calculation on F^2. Programs used to solve and refine the structure were: SHELXS97 and SHELXL97. Molecular graphics; Ortep-3 for windows.[21]

Crystallographic data for the structures reported here have been deposited with the Cambridge Crystallographic Data Centre [Deposition Nos. CCDC-280899 for 2-Cl-dimer (**3**), CCDC-280901 for 3-MeO-4-OH dimer (**17**), and CCDC-280900 for **22**]. The data can be obtained free of charge via www.ccdc.cam.ac.uk/perl/catreq/catreq.cgi (or from the CCDC, 12 Union Road, Cambridge CB2 1EZ, UK; Fax: +44-1223 336033; E-mail: deposit@ccdc.cam.ac.uk).

4.4. Cell culture

MDA-MB-231 (a human breast cancer) and SW620 (a human colon cancer) cell line were originally purchased from ATCC and maintained in RPMI 1640 (Gibco/BRL) containing 10% heat-inactivated fetal bovine serum (hyclone) and 25 mM HEPES. Cells were grown in 37 °C incubator maintained 5% CO_2 under humidified condition and subcultured into a new cell culture dishes per 72 h after detaching the cells with trypsin-EDTA (Gibco/BRL).

4.5. Purification of GST fusion proteins

The bacterial pellet was disrupted by sonication at 4 °C in lysis buffer containing 10 μg/mL aprotinin, 10 μg/mL leupeptin, 100 μg/mL AEBSF, and 10 mM DTT. The homogenate was then centrifuged for 10 min at 4 °C at 10,000*g*. The resulting supernatant fraction was immediately mixed and rotated with glutathione beads (equilibrated with lysis buffer) for 1 h at 4 °C (5 vol of supernatant/1 vol of 50% bead slurry). The glutathione beads were washed two times with 10 vol of lysis buffer and then twice with 10 vol of 2× reaction buffer (60 mM Tris, pH 8.5, 150 mM NaCl, 1.34 mM EDTA, and 0.066% BSA) containing 10 μg/mL aprotinin, 10 μg/mL leupeptin, 100 μg/mL AEBSF, and 10 mM DTT. The fusion protein was eluted with three successive washes using 10 mM glutathione in 2× reaction buffer. Active fractions were pooled and supplemented with 20% glycerol prior to storage at −80 °C (Brisson et al., 2004).[22]

4.6. Dual-specific Cdc25B and phosphatase assay[22]

The activity of the GST fusion Cdc25B or A phosphatase was measured with FDP (Molecular Probes, Inc., Eugene, OR), which is readily metabolized to the fluorescent fluorescein monophosphate, as a substrate in a 96-well microtiter plate. The final incubation mixture (150 μL) comprised of 30 mM Tris (pH 8.5), 75 mM NaCl, 0.67 mM EDTA, 0.033% bovine serum albumin, 1 mM DTT, and 20 μM FDP for Cdc25B or A phosphatase. Inhibitors were resuspended in DMSO, and all reactions including controls were performed at a final concentration of 7% DMSO. Reactions were initiated by adding ~0.25 μg of fusion protein and incubated at ambient temperature for 1 h for Cdc25B phosphatase. Fluorescence emission from the product was measured with a multiwell plate reader (Perseptive Biosystems Cytofluor II, Framingham, MA; excitation filter, 485/20; emission filter, 530/30).

4.7. PTP-1B enzyme assay

In order to carry out PTP-1B counterscreenig, the cDNA encoding the catalytic domain of PTP-1B (residues 1–322) was cloned into the NdeI site of pET14b and expressed in *Escherichia coli* BL21. After overnight culture with 0.1 mM IPTG for induction, the histidine-tagged PTP-1B fusion protein was purified from bacterial lysates by using a nickel-chelated affinity column. The enzyme assay for PTP-1B was carried out on 96-well plates. To each well (final volume: 200 mL) were added 20 AM FDP and 0.1 Ag PTP-1B in a buffer containing 30 mM Tris (pH 8.0), 75 mM NaCl, 0.67 mM EDTA and, 1 mM dithiothreitol with or without test compounds. Following incubation at room temperature for 1 h, the fluorescence released by enzyme catalysis was measured at 485 nm (excitation) and 538 nm (emission) by using a fluorometer (Synergy HT, BioTek).

4.8. Cell proliferation assays

Cells (5000 cells/well) were seeded into 96-well plates in RPMI 1640 containing 10% FBS. After 24 h, each compound diluted with DMSO was treated to each well. Cell proliferation reagent, WST-1 (Roche Applied Science), was added after 24 h. The plate was incubated in 37 °C incubator for 2 h and absorbance was measured at 450 nm using an ELISA Reader (Bio-Rad).

4.9. Cell cycle analysis

Cells were trypsinized at the time after compound treatment and gathered by centrifugation at 300*g* for 5 min at room temperature. Supernatant was discarded and precipitated cells were washed with phosphate-buffered saline. Cells were fixed with ice-cold 70% ethanol

overnight. Fixed cells were centrifuged at 300*g* for 5 min at room temperature and washed twice with phosphate-buffered saline. Cells were diluted with PBS solution (1×10^5 cells/100 μL) and treated with 100 μg/mL RNase A at 37 °C for 30 min. For DNA staining, 50 μg/mL of propidium iodide was added to the cells. Analysis was carried by 20,000 cells with FACScalibur (Becton Dickinson). Cell cycle distribution was analyzed by Modifit's program (Becton Dickinson).

4.10. Western blotting

Cell lysates treated with chemicals were prepared by RIPA lysis buffer (50 mM Tris, pH 7.0, 150 mM NaCl, 5 mM EDTA, 1% Triton X-100, 1% deoxycholic acid, 0.1% SDS, 30 mM Na_2HPO_4, 50 mM NaF, and 1 mM $NaVO_4$) containing protease inhibitor cocktail (Roche Applied Science). Proteins (40 μg) were resolved by 7.5 or 10% SDS–PAGE and transferred to PVDF membrane (Roche Applied Science). The membrane were blocked with 5% nonfat dried milk in TBS-T (50 mM Tris–HCl, pH 7.6, 150 mM NaCl, and 0.1% Tween 20) and probed with primary antibodies (Cell Signaling Technology) for 2–2.5 h. The blot was washed, exposed to HRP-conjugated anti-rabbit IgG for 1.5 h, and examined by chemiluminescence POD reagents (Roche Applied Science).

4.11. Nude-mouse xenograft assay

For the evaluation of compound **21** for antitumor activity in vivo, SW620 human colon adenocarcinoma cells (3×10^7 cells/mL) were implanted subcutaneously into the right flank of nude mice on day 0. Compound was dissolved in acidic water (pH 3) and was intraperitoneously administered at a concentration of 10 mg/kg per day for 20 days. Tumor volumes were estimated as: length (mm) × width (mm) × height (mm). To determine the toxicity of the compound, the body weight of tumor-bearing animals was measured. The mice were sacrificed and the tumors were weighed at day 20.

Acknowledgments

This research was financially supported by grants from Plant Diversity Research Center of 21st Century Frontier Research Program, KRIBB Research Initiative Program, the National Chemical Genomics Research Program, and Center for Biological Modulators (CBM1-B500-001-1-00) of the 21st Century Frontier Research Program.

References and notes

1. Lee, H. S.; Ahn, Y. J. *J. Agric. Food Chem.* **1998**, *46*, 8–12.
2. Kwon, J. A.; Yu, C. B.; Park, H. D. *Lett. Appl. Microbiol.* **2003**, *37*, 61–65.
3. Lee, C. W.; Hong, D. H.; Han, S. B.; Park, S. H.; Kim, H. K.; Kwon, B. M.; Kim, H. M. *Planta Med.* **1999**, *65*, 263–266.
4. Choi, J.; Lee, K. T.; Ka, H.; Jung, W. T.; Jung, H. J.; Park, H. J. *Arch. Pharm. Res.* **2001**, *24*, 418–423.
5. Ka, H.; Park, H. J.; Jung, H. J.; Choi, J. W.; Cho, K. S.; Ha, J.; Lee, K. T. *Cancer Lett.* **2003**, *196*, 143–152.
6. Han, D. C.; Lee, M. Y.; Shin, K. D.; Jeon, S. B.; Kim, J. M.; Son, K. H.; Kim, H. C.; Kim, H. M.; Kwon, B. M. *J. Biol. Chem.* **2004**, *279*, 6911–6920.
7. Kwon, B. M.; Cho, Y. K.; Lee, S. H.; Nam, J. Y.; Bok, S. H.; Chun, S. K.; Kim, J. A.; Lee, I. R. *Planta Med.* **1996**, *62*, 183–184.
8. Kwon, B. M.; Lee, S. H.; Cho, Y. K.; Bok, S. H. *Bioorg. Med. Chem. Lett.* **1997**, *7*, 2473–2476.
9. Jeong, J. H.; Kim, M. R.; So, K. H.; Han, M. Y.; Ha, J. H.; Garnier, M.; Meijer, L.; Kwon, B. M. *Bioorg. Med. Chem. Lett.* **2000**, *10*, 1819–1822.
10. Jeong, H. W.; Han, D. C.; Son, K. H.; Han, M. Y.; Lim, J. S.; Ha, J. H.; Lee, C. W.; Kim, H. M.; Kim, H. C.; Kwon, B. M. *Biochem. Pharmacol.* **2003**, *65*, 1343–1350.
11. Galaktionov, K.; Beach, D. *Science* **1995**, *269*, 1575–1577.
12. Lammer, C.; Wagerer, S.; Saffrich, R.; Mertens, D.; Ansorge, W.; Hoffmann, I. J. *Cell Sci.* **1998**, *111*, 2445–2453.
13. Sadhu, K.; Reed, S. I.; Richardson, H.; Russell, P. *Proc. Natl. Acad. Sci. U.S.A.* **1990**, 5139–5143.
14. Galaktionov, K.; Beach, D. *Cell* **1991**, *67*, 1181–1194.
15. Nagata, A.; Igarashi, M.; Jinno, S.; Suto, K.; Okayama, H. *New Biol.* **1991**, *3*, 959–968.
16. Millar, J. B.; Blevitt, J.; Gerace, L.; Sadhu, K.; Featherstone, C.; Russell, P. *Proc. Natl. Acad. Sci. U.S.A.* **1991**, *88*, 10500–10504.
17. Jinno, S.; Suto, J.; Nagata, A.; Igarashi, M.; Kanaoka, Y.; Nojima, H.; Okayama, H. *EMBO J.* **1994**, *13*, 1549–1556.
18. Nilsson, I.; Hoffmann, I. *Prog. Cell Cycle Res.* **2000**, *4*, 107–114.
19. Wehbe, M.; Peyrot, M.; Lepage, L.; LePage, Y. *Bull. Soc. Chim. Fr.* **1982**, 321–322.
20. El Gendy, A. M.; Mallouli, A.; Lepage, Y. *Synthesis* **1980**, 898–899.
21. Sheldrick, G. M. SHELXS97 and SHELXL97, Program for the Refinement of Crystal Structures, University of Göttingen, Germany, 1997.
22. Brisson, M.; Nguyen, T.; Vogt, A.; Yalowich, J.; Giorgianni, A.; Tobi, D.; Bahr, I.; Stephenson, C. R. J.; Wipf, P.; Lazo, J. S. *Mol. Pharm.* **2004**, *66*, 824–833.